The effect of RKKY interactions on the magnetization of dilute magnetic alloys with hcp hosts*

P. Gash,† R. Roshko,†† and O. G. Symko

Department of Physics, University of Utah, Salt Lake City, Utah 84112

The magnetization due to the presence of magnetic impurities dissolved dilutely in nonmagnetic H.C.P. host metals has been calculated assuming a fine structure splitting by an axially symmetric crystal field and an RKKY interaction between the impurities. To compute the RKKY contribution, the interaction between the impurities is described by a randomly oriented effective internal exchange field H with a probability distribution $P(\vec{H}) = \Delta/\pi^2(\Delta^2 + H^2)^2$. Comparison of the calculated magnetization with the measured magnetization of a 5 ppm single crystal of MgMn and several polycrystalline ZnMn samples of varying concentration, over the temperature range 2K to 10mK, yields estimates for Δ, the most probable value of the magnitude of the effective exchange field, as well as the dependence of Δ on impurity concentration.

PACS numbers: 71.70. – d

INTRODUCTION

Recent low-temperature magnetization measurements [1,2,3] on very dilute (<100 ppm) magnetic systems such as MgMn, ZnMn, and ZnCr have shown that the crystal field of the host can play a substantial role in determining the magnetic behaviour of the impurity. In addition to such single-impurity effects, these measurements also reveal the presence of a concentration-dependent interaction which causes the magnetization per impurity to decrease with increasing impurity concentration, and which is attributed to an RKKY-type coupling between the magnetic impurities. In this paper, we present a simple physical model for dilute magnetic alloys consisting of 3d transition impurities dissolved in H.C.P. host metals which can account for the measured magnetization in such systems and which incorporates both crystal field theory and the molecular field theory of spin glasses.

THEORY

The model Hamiltonian for one impurity contains contributions from three sources: the external field, the internal RKKY field, and the crystal field. Figure 1 shows the relative orientation of the external field $\vec{H}_0$, the internal field $\vec{H}$, and the c-axis of the crystal.

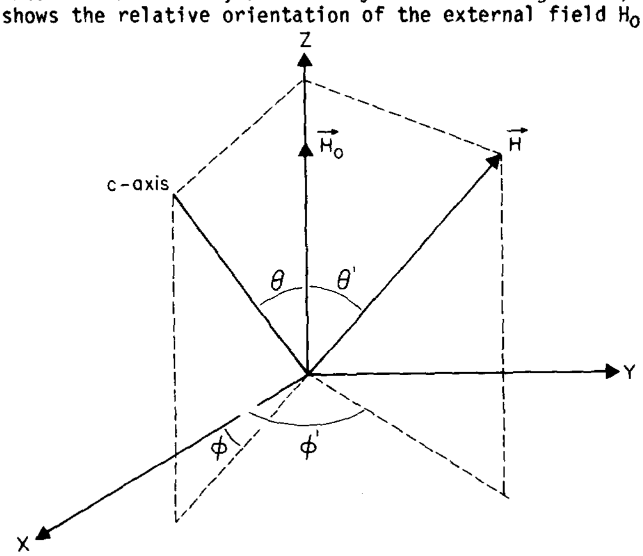

FIG. 1 - The relative orientations of the external field $\vec{H}_0$, the internal field $\vec{H}$, and the c-axis of the crystal.

The orbital angular momentum of the impurity is assumed to be quenched by the crystal field of the host, and hence the impurity is represented by an effective spin $\vec{S}$. Under these conditions, the effect of spin-orbit coupling is to partially restore the quenched orbital angular momentum, resulting in a fine-structure splitting of the spin multiplet which, in the principal axis system of the crystal and for axial symmetry, has the form [4] $D[S_{\xi}^2 - S(S+1)/3]$. In the xyz coordinate system in Fig. 1, the fine-structure splitting term in the Hamiltonian depends on θ and φ. The RKKY interaction between the impurities is assumed to be a Heisenberg exchange interaction, $\sum_{i,j} J_{ij}\vec{S}_i\cdot\vec{S}_j$, and is represented by an effective internal exchange field which, for the ith impurity site, has the form $\vec{H}_i = \sum_j J_{ij}\vec{S}_j$. The oscillatory nature of the coupling constant J_{ij} combined with the randomness in the positions of the impurities means that the internal field is a random variable describable by a probability distribution which, for a Heisenberg interaction, has the form [5] $P(\vec{H}) = \Delta/\pi^2(\Delta^2 + H^2)^2$. The parameter Δ corresponds to the most probable value of the magnitude of the internal field. Both the internal and external field terms in the Hamiltonian have the form of a Zeeman interaction: $g\mu_B\vec{S}\cdot\vec{H}_0$ and $g\mu_B\vec{S}\cdot\vec{H}_i$.

If the eigenstates and eigenvalues of the Hamiltonian are known then the thermal average of the magnetic moment per impurity along the external field direction (z) can be computed from the expression $\bar{\mu} = \sum_n \langle n|g\mu_B S_z|n\rangle \exp(-E_n/k_BT)/\sum_n \exp(-E_n/k_BT)$, where $|n\rangle$ and E_n are the eigenstates and eigenvalues of the Hamiltonian, respectively. For a single crystal, θ and φ are constants, and the magnetization is obtained by averaging $\bar{\mu}$ over all possible values of the internal field using the above distribution:

$$M(\text{single crystal}) = Nc \int \bar{\mu}\, P(\vec{H})d\vec{H}, \tag{1}$$

where N is the number of lattice sites per unit volume in the host and c is the fractional impurity concentration. For a polycrystalline sample, an additional average must be performed over all possible orientations of the crystallites (i.e., over θ and φ):

 0021-8979/81/031720-03$1.10

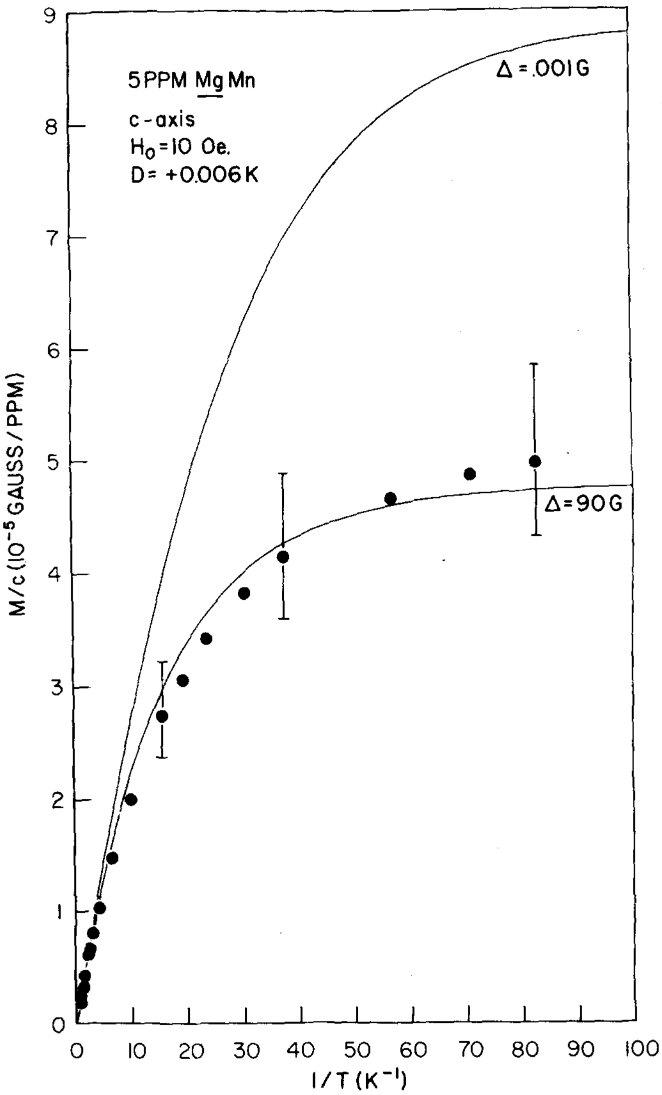

FIG. 2 - The magnetization along the c-axis of a 5 ppm single crystal of MgMn.

$$M(\text{polycrystal}) = \int_0^{2\pi}\int_0^{\pi/2} M(\text{single crystal})\, P(\theta,\phi)\, d\theta d\phi, \quad (2)$$

where $P(\theta,\phi) = \sin\theta/2\pi$ and M(single crystal) is given by Eq. (1). All the integrals appearing in Eqs. (1) and (2) were evaluated using the Gauss-Legendre quadrature and the upper limit of infinity on the H-integral was replaced by a finite value L such that the distribution $P(\vec{H})$ was normalized to 0.99.

APPLICATIONS

The expressions for the magnetization derived above were applied to two different systems: single crystal MgMn and polycrystalline ZnMn. The values of the effective impurity spin S and the crystal field parameter D used in the present calculation were obtained from a previous analysis [2,3] of both systems which was based on a Spin Hamiltonian similar to that discussed above but containing only the crystal field and external field terms (no RKKY term). For MgMn, S=5/2 (assuming g=2) and D=+0.006K, while for the ZnMn system, S=1 and D=-0.070K.

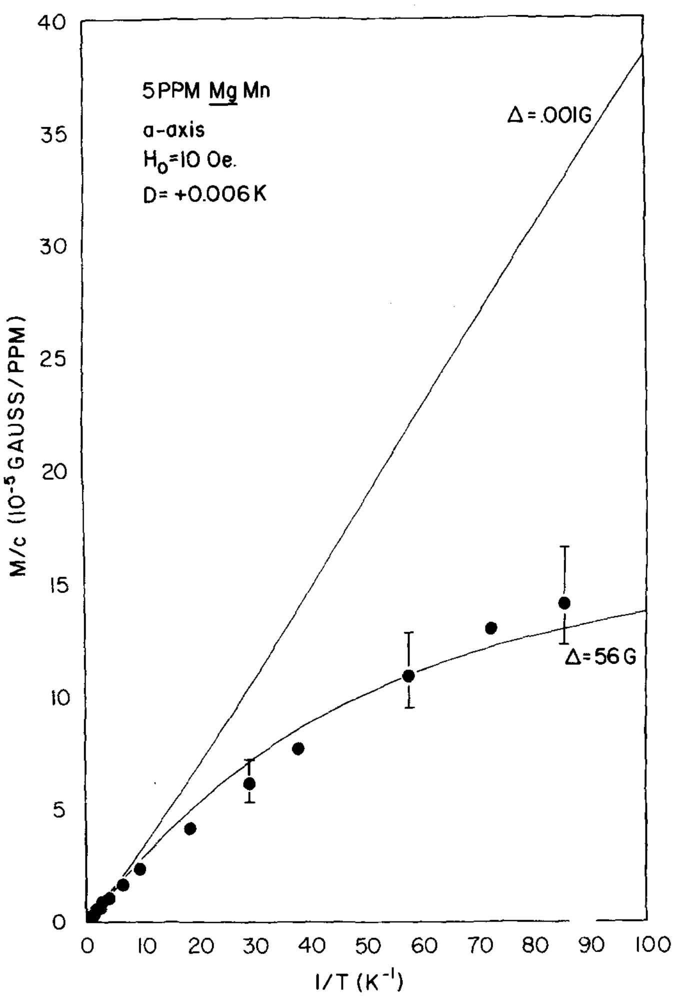

FIG. 3 - The magnetization along the a-axis of a 5 ppm single crystal of MgMn.

(a) Single Crystal MgMn

Figure 2 shows the magnetization per ppm of impurity along the c-axis of a 5 ppm single crystal of MgMn, plotted as a function of 1/T. The solid curves represent the calculated c-axis magnetization, while the error bars on the data points correspond to an estimated error of ±15% in the analyzed Mn concentration. For the c-axis magnetization, the appropriate Hamiltonian is obtained by setting $\theta=0$ and $\phi=0$ so that the direction of the external field coincides with that of the symmetry axis (see Fig. 1). The solid curves in Fig. 2 were obtained by diagonalizing the associated 6x6 matrix for S=5/2 and D = +0.006K to obtain the eigenvalues and eigenvectors, and using Eq. (1) to calculate the magnetization. The curve for Δ = .001G illustrates the effect of the crystal field in the absence of any internal RKKY field, while the curve for Δ = 90G provides the best fit to the experimental data. Similar fits to the data points corresponding to the extreme ends of the error bars in Fig. 2 yield lower and upper bounds for Δ of 56G and 125G, respectively.

For the a-axis magnetization shown in Fig. 3, where the external field lies in the plane perpendicular to the symmetry axis of the crystal, the appropriate Hamiltonian is obtained by setting $\theta = \pi/2$ and $\phi = 0$, and a similar treatment of the data yields a best-fit value for Δ along the a-axis of Δ =56G, with lower and upper bounds of 40G and 75G, respectively. The values for Δ_c and Δ_a thus overlap within experimental error, implying that the exchange interaction between the impurity spins is isotropic.

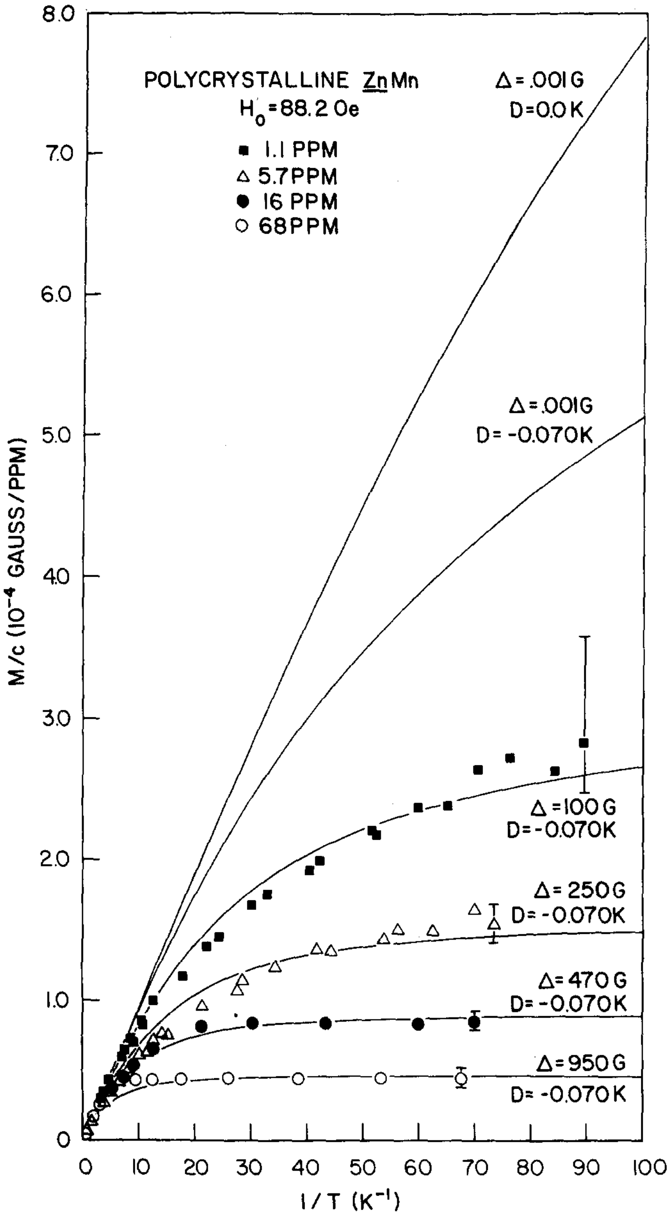

FIG. 4 - The magnetization for polycrystalline ZnMn.

(b) Polycrystalline ZnMn

Figure 4 shows the magnetization per ppm of impurity, in an external field H_0 = 88.2 Oe, plotted as a function of 1/T for several polycrystalline samples of ZnMn of varying concentration. As before, the solid curves represent the calculated magnetization for various values of D and Δ, while the error bars on the data points correspond to the following concentration errors: c = 1.1 ± 0.2 ppm, 5.7 ± 0.5 ppm, 16 ± 1 ppm, and 68 ± 7 ppm. For a polycrystalline system, θ and ϕ are now variables, and the magnetization was calculated using Eq. (2) and the eigenvectors and eigenvalues obtained by diagonalizing the 3x3 matrix representing the Spin Hamiltonian for S = 1.

The curve for D = 0K and Δ = .001G in Fig. 4 shows the magnetization for a system of free impurity spins in the limit of zero crystal field and a negligible internal field, while the curve for D = -0.070K and Δ = .001G illustrates the effect of the crystal field appropriate to ZnMn (averaged over all the crystallites) for a vanishingly small internal field. The remaining curves for D = -0.070K and Δ = 100G, 250G, 470G, and 950G represent the best fits to the experi-

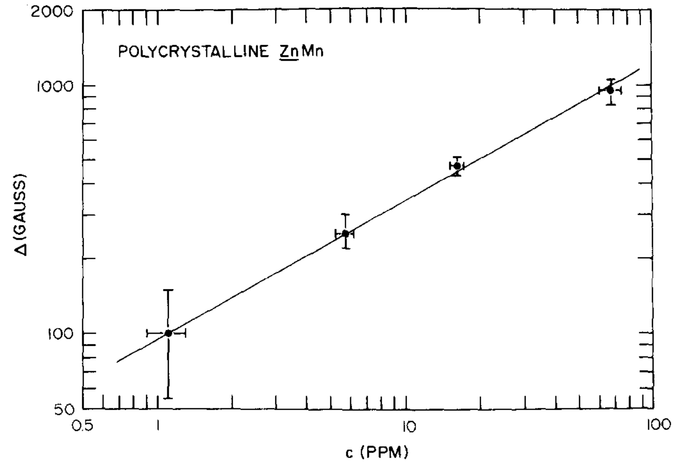

FIG. 5 - The most probable internal field Δ as a function of impurity concentration c for polycrystalline ZnMn.

mental data. In Fig. 5, the best-fit values for Δ, the most probable internal field, are plotted as a function of the fractional impurity concentration c (in ppm) on a log-log scale. Molecular field theories of spin glasses predict various concentration dependences for Δ: for the 3-D Heisenberg model, with the internal field distribution discussed in the THEORY, Δ varies linearly with concentration [5], while, for the 1-D Ising model, Klein [6] has shown that the probability distribution has the form of a Lorentzian for small internal fields with $\Delta\alpha c$ and a Gaussian for high internal fields with $\Delta\alpha c^{1/2}$. For the ZnMn system, the straight line in Fig. 5 corresponds to a concentration dependence of c^n with $n = 0.56^{+.07}_{-.15}$, implying that the Ising model may provide a more appropriate description of spin glass behaviour then the Heisenberg model.

REFERENCES

*Support by NSF DMR-79-16243
†Permanent address: Natural Science Division, Shasta Community College, Redding, CA.
††Postdoctoral Fellow of the Natural Sciences and Engineering Research Council of Canada.
1. J.C. Doran, S.F. Kral, T. Steelhammer, and O.G. Symko, Solid State Comm. 17, 1099 (1975).
2. S.F. Kral, L.A. Moberly, T. Steelhammer and O.G. Symko, Solid State Comm. 32, 671 (1979).
3. L. Moberly, R. Roshko, and O.G. Symko, Bull. Am. Phys. Soc., Vol. 25, No. 3, p. 306 (1980).
4. A. Abragam and B. Bleaney, Electron Paramagnetic Resonance of Transition Ions, Clarendon Press, Oxford, 1970, p. 157.
5. L.R. Walker and R.E. Waltstedt, Phys. Rev. (to be published).
6. M.W. Klein, Phys. Rev. B 14, 5008 (1976).